Proc. Natl. Acad. Sci. USA
Vol. 87, pp. 3405–3409, May 1990
Biophysics

Supramolecular arrangement of *Rhodospirillum rubrum* B880 holochrome as studied by radiation inactivation and electron paramagnetic resonance

(bacterial photosynthesis/bacteriochlorophyll/antenna proteins)

GABRIEL GINGRAS* AND RAFAEL PICOREL†

Département de Biochimie, Université de Montréal, Case Postale 6128A, Montréal, PQ, H3C 3J7 Canada

Communicated by Joseph J. Katz, February 9, 1990 (received for review December 7, 1988)

ABSTRACT **Oxidation of the B880 antenna holochrome gives rise to a 3.8-G linewidth electron paramagnetic resonance (EPR) signal that is considerably narrower than the 13-G signal of monomeric bacteriochlorophyll (Bchl) cation. Radiation inactivation was used to verify a model according to which this linewidth narrowing is due to delocalization over several Bchl molecules. Chromatophores of the photoreaction centerless mutant F24 of *Rhodospirillum rubrum* were subjected to different doses of γ-radiation. This induced not only a decay of the EPR signal amplitude but also its linewidth broadening. According to target theory, the induced amplitude decay of the EPR signal had a target size of 10.5 kDa. This is attributed to an elementary structure ($\alpha_1\beta_1$Bchl$_2$), whose number in the membrane would limit the rate of encounter with ferricyanide and thus the formation of unpaired spins. We applied Bernoulli statistics to predict, for a given survival probability of the signal, the number of surviving elementary structures in aggregates of ($\alpha_1\beta_1$Bchl$_2$)$_n$ where n was varied from 4 to 7. Using an equation that predicted the Bchl special pair in the photoreaction center, we were able to simulate the observed relationship between the EPR linewidth and the dose of radiation. The best fit was obtained with a hexameric structure ($\alpha_1\beta_1$Bchl$_2$)$_6$.**

The antenna chlorophyll of photosynthetic organisms is noncovalently bound to specific intrinsic membrane proteins. The light energy it absorbs is transferred to the photoreaction center and transformed into an oxidation–reduction potential. The chlorophyll–chlorophyll and chlorophyll–protein molecular interactions modulate the absorption spectra of the antennas, thus playing an important role in determining the ecological habitat of their host organisms. In the bacteriochlorophyll (Bchl) a-containing purple bacteria, there are two main groups of protein–Bchl complexes or "holochromes": the B800–B850 and the B880 holochromes, so designated after their peak absorption wavelengths in the near-infrared (1–3). This article is concerned with the second of these complexes, the B880 holochrome.

In recent years, the B880 holochromes from a few photosynthetic bacteria have been isolated and characterized. That of *Rhodospirillum rubrum*, as judged by its absorption spectrum (4, 5), has been obtained in a native form. It contains Bchl and spirilloxanthin (Spir) in a 2:1 (mol/mol) ratio and is copurified with small amounts of mono- and diphosphatidylglycerol and of phosphatidylethanolamine. Its protein moiety consists of two different polypeptides present in a 1:1 (mol/mol) ratio (4, 5) whose exact molecular weights of 6079 and 6101 can be deduced from their amino acid sequences (6–8). The mRNA encoding this B880 holochrome has been isolated and its genes have been cloned and sequenced (9, 10).

The publication costs of this article were defrayed in part by page charge payment. This article must therefore be hereby marked "*advertisement*" in accordance with 18 U.S.C. §1734 solely to indicate this fact.

Essential as they are, the above data provide little direct information about localization of the pigments on the polypeptides or about the type of pigment–pigment or pigment–protein interaction in the holochrome. In a different approach, we used the radiation inactivation technique to estimate the *in situ* molecular size of the structures associated with different properties of the holochrome. Making use of the fact that *Rs. rubrum* contains only the B880 holochrome, we applied target analysis to γ-irradiated photoreaction centerless chromatophores (11). While the target size for inactivation of Bchl assayed in organic solvent extracts was 7 kDa, we found that Spir, the 880-nm band, and the oxidation-induced 1225-nm band have the same target size of 13–14 kDa. The latter target size was attributed to a ($\alpha_1\beta_1$Spir$_1$-Bchl$_2$) structure in which the Bchl–Bchl interaction is disrupted whenever one of the two 7-kDA polypeptide–pigment complexes is destroyed. This further suggests that each one of the two polypeptides carries one Bchl molecule and that the binding site of Spir is shared between the two polypeptides. The interaction of the two Bchl molecules would give rise to the 880-nm absorption band and, after oxidation, to the 1225-nm absorption band (11).

From a different viewpoint, chemical cross-linking, isolation, and molecular sizing of particles as well as electron paramagnetic resonance (EPR) data have been interpreted to mean that the B880 holochrome may form large aggregates in the membrane (12–17). Resolution, according to their size, of complexes with absorption peaks at wavelengths from 775 to 873 nm is in favor of that hypothesis (15, 16). For our part, we have attributed the line narrowing in the EPR spectra of oxidized B880 Bchl, either in the chromatophores or in isolated complexes, to hexameric structures containing 12 Bchl molecules (17, ‡). The present work is an attempt to verify this model by applying target analysis to study the oxidation-induced EPR signal in γ-irradiated photoreaction centerless chromatophores. The rationale of this experiment was that if indeed the holochrome forms large and isolated oligomers of homogeneous size, their partial destruction by γ-irradiation should produce a predictable statistical distribution of surviving oligomers of various sizes and Bchl contents. As a consequence, one would expect not only a decreased amplitude but also a linewidth variation of the EPR signal as a function of the dose of irradiation. We found this prediction verified.

Abbreviations: Bchl, bacteriochlorophyll; Spir, spirilloxanthin; EPR, electron paramagnetic resonance.

*To whom reprint requests should be addressed.
†Present address: Consejo Superior de Investigaciones Cientificas, Estacion Experimental de Aula Dei, Montanana, 177 (Aula Dei), 50016 Zaragoza, Spain.

‡Gingras, G., Picorel, R. & Norris, J. M., Workshop on Molecular Structure and Function of Light-Harvesting Pigment-Protein Complexes and Photosynthetic Reaction Centers, July, 1983, Eidgenossiche Technische Hochschule, Zurich, abstr. I-7.

MATERIALS AND METHODS

Biological Material. Photoreaction centerless *Rs. rubrum* strain F24 (18) was grown in the synthetic medium of Lascelles (19) supplemented with 2 g of yeast extract per liter (Difco). The cells were cultured aerobically in the dark at 32°C in 2-liter flasks filled to ≈80% of their capacity in a rotatory shaker (New Brunswick Scientific). The deep purple cells were harvested 18 hr after inoculation, near their stationary growth phase. After one washing with distilled water, the cells were kept frozen at −20°C. Chromatophores were extracted by alumina grinding followed by centrifugation (20), dispersed in 50 mM sodium phosphate (pH 7.0), and kept in the dark at 4°C for a maximum of 2 days before use.

Irradiation and Target Analysis. For each experiment, 24 Eppendorf microcentrifuge tubes (1.5 ml) containing 0.5 ml of chromatophores (A_{880} = 10) were lyophilized in a Speed Vac concentrator (Savant) at a pressure of 4–5.3 Pa for at least 5 hr to ensure complete dryness of the samples. The tubes were flushed with ultradry nitrogen gas before capping and were placed in a specially designed tube rack allowing isodose exposure (21). They were irradiated in the cylindrical chamber of a Gammacell 220 ^{60}Co irradiator (Atomic Energy of Canada, Ottawa) giving ≈3 Mrad of γ-radiation per hr (1 rad = 0.01 Gy). Exposure to radiation was carried out at a uniform temperature of 38°C. Sets of three tubes were exposed to the same radiation dose to yield an average value of inactivation.

EPR Spectroscopy. Dry chromatophore samples were dispersed in deionized water. After addition of potassium ferricyanide, their EPR spectra were recorded in a Varian E-line century spectrometer operating at a microwave frequency of 9.4 GHz in an E-231 cavity. The modulation frequency of the magnetic field was 100 kHz. The spectra were recorded at room temperature in flat quartz cells. Before recording the spectra, the microwave power was systematically varied to avoid possible saturation artifacts. Under our experimental conditions, the signal showed no sign of saturation until well above 10 mW. All the experiments reported here were performed at power levels of 5 mW or less. Similarly, the modulation amplitude was varied to check possible line broadening due to excessive modulation amplitude; a modulation amplitude of 2 G (2×10^{-4} T) was used throughout. No signal was observed in the absence of added ferricyanide, whether the samples were irradiated or not.

Since the absorption spectra were gaussian curves, the relative number of unpaired spins were calculated from the recording of the first derivative spectra, using the relationship

$$\int_{-\infty}^{+\infty} Y dH = Y_{max} \Delta H_{pp} (\pi/2)^{1/2}, \quad [1]$$

where Y is the microwave absorption at a given magnetic field, H; Y_{max} is the peak absorption value; and ΔH_{pp} is the peak to peak linewidth obtained from the derivative spectrum. Y_{max} was obtained by graphic integration of the derivative spectrum, since

$$Y_{max} = \int_{H_0}^{H_r} Y' dH, \quad [2]$$

where $Y' = dy/dH$ is the first derivative EPR line and H_r is the magnetic field value of resonance.

RESULTS AND ANALYSIS OF THE DATA

Treatment of photoreaction centerless chromatophores with ferricyanide produces a bleaching of the 880-nm absorption band and the appearance of an absorption band at 1225 nm that is due to oxidation of the B880 holochrome Bchl. Concomitantly with these optical changes, oxidation of the holochrome Bchl is associated with an EPR signal of gaussian lineshape and with a g value of 2.0025, consistent with free electron delocalization over the large Bchl macrocycle. In fresh chromatophores, the peak to peak derivative linewidth of this signal is 3.8 G (17) rather than 13 G as would be expected for oxidized monomeric Bchl (22). Moreover, the peak to peak linewidth of 99.9% deuterated holochrome was 1.8 G (‡) instead of 5.4 G (23). This linewidth narrowing was suggested earlier to be due to hyperfine interaction, indicating extensive delocalization of the unpaired electron over several Bchl molecules (17, ‡).

Fig. 1 shows the relative number of spins in a chromatophore suspension as a function of the ferricyanide/Bchl molar ratio. The signal intensity is not saturated until well above a ferricyanide concentration of 200 mM, where the relative number of spins was normalized. This curve is typical of a one-site binding isotherm. A ferricyanide concentration of 100 mM corresponding to a ferricyanide/Bchl molar ratio of 1400 was used throughout this work.

Fig. 2 shows that after the chromatophores have been lyophilized and subjected to γ-irradiation, destruction of the holochrome produces not only a decrease in the peak to peak amplitude but also a linewidth broadening of the EPR signal. The rest of this article will deal with these two different aspects of the EPR spectra.

Target Size Associated with the EPR Signal. To calculate the target size of the structure associated with the EPR signal, we used the function

$$N/N_0 = \exp(-\sigma D), \quad [3]$$

where N is the relative number of unpaired spins due to oxidized holochrome molecules before (N_0) and after (N) receiving a certain dose of radiation (D) expressed in Mrad (10^8 erg/g). By definition, the target cross-section $\sigma = 1/D_{37}$, where D_{37} is the dose required to diminish the relative number of unpaired spins to 37% of its initial value. We used the proportionality factor $M_r = 6.4 \times 10^5/D_{37}$ as established empirically by Kepner and Macey (24). Fig. 3 is a semilogarithmic plot of the residual EPR signal (N/N_0) as a function of the dose received by the chromatophores. Analysis of the experimental curve (continuous line) by the least-squares method yields a target size of 10,500, close within experimental error to the sum of the M_r of polypeptides α and β (12,180). The dotted line in Fig. 3 is a theoretical curve pertaining to a

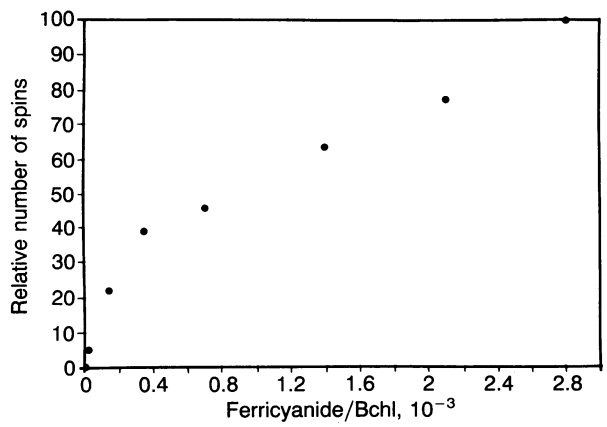

FIG. 1. Relative number of spins in *Rs. rubrum* (F24) chromatophores as a function of the ferricyanide/Bchl molar ratio. The chromatophores were suspended in 50 mM sodium phosphate (pH 7.0). The spectra were recorded at room temperature at 9.4 GHz. Microwave power was 5 mW and modulation amplitude of the magnetic field was 2 G.

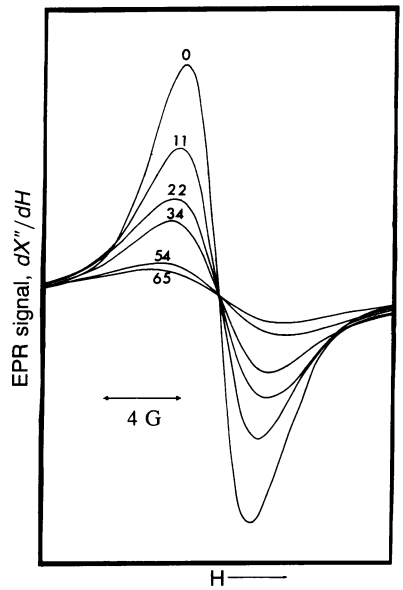

FIG. 2. EPR spectra of the B880 holochrome measured in lyophilized chromatophores of photoreaction centerless *Rs. rubrum* (F24). The samples, in 50 mM sodium phosphate (pH 7.0), were kept oxidized by means of 100 mM potassium ferricyanide (final concentration). The spectra were recorded at room temperature at 9.4 GHz. Microwave power was 5 mW and modulation amplitude of the magnetic field was 2 G. The spectra were recorded in samples exposed to different doses of γ-radiation indicated in Mrad above the corresponding curves.

model of spin delocalization in a hexameric protein structure containing 12 Bchl molecules. This is discussed below.

Analysis of the Linewidth Broadening Caused by Irradiation. Fig. 2 shows that the peak to peak linewidth of the EPR signal is inversely proportional to its survival probability in

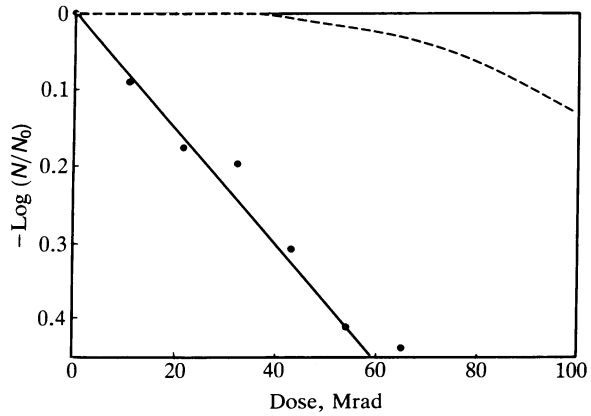

FIG. 3. Radiation inactivation decay of the number of spins of the $g = 2.0025$ EPR signal in photoreaction centerless *Rs. rubrum* (F24) chromatophores. The chromatophores were suspended in 50 mM sodium phosphate (pH 7.0) before lyophilization and irradiation. The experimental values (dots) are the averages of three experiments; the solid line is a least-squares fit of these values. The irradiated samples were kept oxidized by means of 100 mM potassium ferricyanide (final concentration). The spectra were recorded at room temperature at 9.4 GHz. Microwave power was 5 mW and modulation amplitude of the magnetic field was 2 G. The dotted line is a theoretical curve for structure $(\alpha_1\beta_1\mathrm{Spir}_1\mathrm{Bchl}_2)_6$. This was calculated from the following relationship derived from Eqs. **3** and **5** in the text: $N/N_0 = \Sigma_{k=1}^{6} P_6(k) = \Sigma_{k=1}^{6}[\ ]_k^6 p^k q^{n-k}$, where N/N_0, the survival probability of the signal is equated to the sum of the survival probability of oligomers of any size generated by γ-irradiation from structure $(\alpha_1\beta_1\mathrm{Spir}_1\mathrm{Bchl}_2)_6$. The dose, D, was calculated from $p = \exp(-\sigma D)$ (Eq. **3**) taking target cross-section $\sigma = (10{,}500/6.4 \times 10^5)$.

irradiated chromatophores. The following proposes a model relating these two parameters.

First we attempt to account for the spectra obtained in intact chromatophores. We assume that the EPR peak to peak linewidth can be described by the equation proposed by Norris *et al.* (23) to explain the linewidth narrowing in the photoreaction center of photosynthetic bacteria. In this model, the number, Nb, of Bchl molecules over which the unpaired electron is delocalized is given by

$$Nb = (\Delta H_m/\Delta H_n)^2, \quad [4]$$

where ΔH_m is the peak to peak linewidth of monomeric Bchl cation and ΔH_n is the peak to peak linewidth of the signal. Using a value of 13 G for monomeric Bchl cation (22) and 3.75 G for the signal observed (18), we find that $Nb = 12$.

The EPR signal target size and linewidth broadening in γ-irradiated holochrome can be described by a model based on the following conditions or assumptions: (*i*) The holochrome forms aggregates $(\alpha_1\beta_1\mathrm{Spir}_1\mathrm{Bchl}_2)_n$ composed of a definite number, n, of elementary structures $(\alpha_1\beta_1\mathrm{Spir}_1\mathrm{Bchl}_2)$. (*ii*) It is this elementary structure that confers Bchl a midpoint redox potential of $\approx$570 mV such that it can be converted to a cation under our experimental conditions (17). (*iii*) The unpaired electron spin of cationic Bchl is delocalized over (and is confined to) the n $(\mathrm{Bchl})_2$ units contained within each of the aggregates. (*iv*) It thus gives rise to an EPR signal whose linewidth can be described by Eq. **4**. (*v*) After absorbing γ-radiation, an elementary structure does not transfer destructive energy to its neighbors either within or without the larger aggregate.

A consequence of the above assumptions is that after γ-irradiation, chromatophores are predicted no longer to contain a homogeneous population of holochrome aggregates. Instead, this population will now have become heterogeneous in the sense that it will be a statistical distribution of aggregates containing different proportions of intact elementary structures. Moreover, the statistical distribution is expected to vary according to the overall fraction of surviving holochrome.

This statistical distribution of surviving elements can be described by the Bernoulli equation:

$$P_n(k) = \begin{bmatrix} n \\ k \end{bmatrix} p^k q^{n-k}, \quad [5]$$

where $P_n(k)$ is the probability of having k surviving elements in an aggregate constituted of n elementary structures, p is the survival probability of the elementary structures, and $q = 1 - p$ is the corresponding probability of destruction. With Eq. **5**, it is possible to calculate the proportion of $k = 1, 2, \ldots n$ elementary structures surviving for any given survival probability, p. In any given situation, the equation for the first derivative EPR line, Y', is the sum of the spectra of all the surviving elements

$$Y' = -p' \sum_{k=1}^{n} P_n(k) Y_k [4(H - H_r)/\Delta H_k^2] \exp[-2(H - H_r)^2/\Delta H_k^2], \quad [6]$$

where p', the survival probability of the signal, was varied between 0.05 and 1 concomitantly with p^k to better simulate the observed signal decrease after irradiation. Y_k is the peak amplitude, H is the experimental magnetic field value, H_r is the magnetic field of resonance, and ΔH_k is the peak to peak linewidth of the signal when the unpaired spin is delocalized over k elements each containing 2 Bchl molecules. ΔH_k is calculated from Eq. **4** and

$$Y_k = (2/\pi)^{1/2}/\Delta H_k. \quad [7]$$

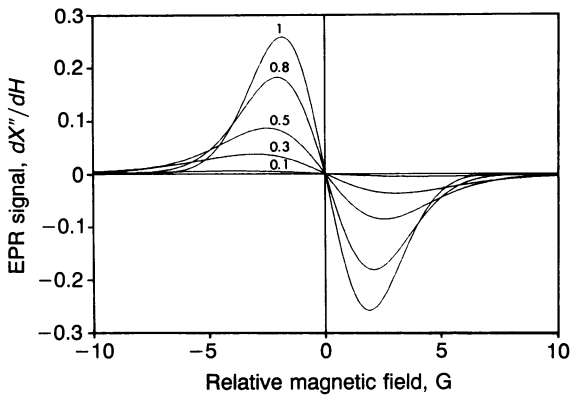

FIG. 4. Simulated EPR spectra of a B880 holochrome consisting of an aggregate of the type $(\alpha_1\beta_1 Spir_1 Bchl_2)_6$. In this simulation, the sample was assumed to have received different doses of γ-radiation leading to EPR signal survival probabilities indicated above the simulated spectra. Simulation was carried out using Eqs. 4–7 in the text.

Fig. 4, based on Eqs. 4–7, is a simulation of the EPR spectra for a set of six elementary structures each containing two Bchl molecules. The equations clearly predict not only a decreased amplitude but also an increasing linewidth of the signal as the survival probability of the signal diminishes. The resemblance of Fig. 4 with the experimental curves of Fig. 2 indicates that our model at least qualitatively predicts the amplitude and linewidth variation of the EPR signal as a function of the dose.

To quantitatively evaluate the correctness of the fit, we compared the EPR signal linewidths measured in samples exposed to different doses of radiation with the linewidths calculated from Eqs. 4–7 for increasing survival probabilities. This comparison is shown with four hypothetical structures of the large aggregate $(\alpha_1\beta_1 Spir_1 Bchl_2)_n$ where n is varied from 4 to 7. Fig. 5 is a plot of linewidth against survival probability p. The experimental values are indicated by dots and the predicted linewidths are shown by solid lines. According to this figure, the fit is best for $n = 5$ (10 Bchl molecules).

The experimental linewidths were found to vary somewhat after lyophilization of the chromatophores, the step preceding γ-irradiation. Whereas fresh chromatophores exhibited linewidths of 3.8 G, lyophilized chromatophores had linewidths of 4.1 G. To keep in line with the initial hypothesis, we interpret this effect of lyophilization as a slight reorganization of the aggregated structure. Since this factor could not be taken into account in our calculations, we multiplied all the values by 3.8/4.1 as a correction. Comparing these corrected values with the predicted curves (Fig. 5), we find a best fit with the hexamer containing 6 copies of each subunit and 12 Bchl molecules.

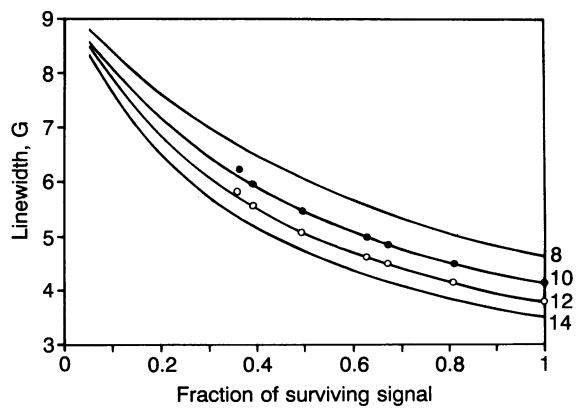

FIG. 5. EPR peak-to-peak linewidth as a function of survival probability of the number of spins in *Rs. rubrum* F24 chromatophores irradiated with γ-rays. Chromatophores were suspended in 50 mM sodium phosphate (pH 7.0) before lyophilization and irradiation. The solid circles are the averages of three experiments and the open circles are the same values corrected for linewidth broadening after lyophilization (see text). The solid lines are simulations according to Eqs. 4–7 of the text. The numbers on the right represent the number of Bchl molecules assumed to be present in the aggregate $(\alpha_1\beta_1 Spir_1 Bchl_2)_n$.

DISCUSSION

In a previous study (17) we inferred, by analogy with the 1250-nm band of the oxidized photoreaction center, that the oxidation-induced 1225-nm band of the B880 holochrome is probably due to a pair of Bchl molecules. The correctness of that deduction was shown by target analysis of the 880-nm and 1225-nm absorption bands in photoreaction centerless chromatophores (11). Whereas the target size for Bchl in the chromatophores is 7 kDa, that of the 880-nm and 1225-nm bands is 14 kDa, indicating that a single hit within a structure composed of 2 polypeptides, of 1 Spir and 2 Bchl molecules is sufficient to destroy the molecular interaction responsible for these bands. Since a 7-kDa Bchl-carrying species, attributed to a residual polypeptide, is left after this hit, there obviously is no transfer of destructive energy between the α and β polypeptides (11).

Another previous deduction was that the oxidation-induced 1225-nm band and EPR signal, having the same midpoint redox potential of 570 mV, probably arise from the same chemical species (17). This interpretation is strongly supported (Fig. 3) by the similarity within experimental error of their target sizes, respectively, of 14 and 10.5 kDa. The latter value is almost certainly the least accurate of the two due to imprecision in determining the relative number of spins.

The target size of the EPR signal precludes that the destructive energy of the γ-radiation could be transferred among the elementary structures. It might, therefore, be thought to follow that the unpaired electron spin must be confined to the two Bchl molecules of this elementary structure. In that case, however, Eq. 4 would predict a linewidth of 9.2 G for the EPR signal instead of the observed 3.8 G. Such a discrepancy might only mean that Eq. 4, in spite of its predictive value for the Bchl special pair of the bacterial photoreaction center (25) as verified by x-ray crystallography (26, 27), does not apply to the B880 holochrome. It would not be surprising if this equation were not of general applicability, as illustrated by the chlorophyll a-containing primary electron donor of plant photosystem I (28, 29).

This apparent difficulty in applying Eq. 4 can be overcome by assuming that (*i*) the destructive γ-radiation energy is not transferred among the elementary structures, which thus are destroyed one by one with a probability described by their target size and (*ii*) that the elementary structures form larger aggregates, $(\alpha_1\beta_1 Spir_1 Bchl_2)_n$, allowing the unpaired electron spin to be delocalized over n $(Bchl)_2$ units. Then, the piecemeal γ-ray destruction of the elementary structures would produce not only an overall decrease in the EPR signal but also its line broadening. This line broadening would be due to the increasing proportion of aggregates containing a smaller than normal population of $(Bchl)_2$ units.

The best justification of this model is that it correctly predicts the line broadening of the signal as a function of survival probability (Figs. 2, 4, and 5). Eq. 4, therefore, correctly describes the linewidth of the EPR signal as due to electron spin delocalization over 12 Bchl molecules. Moreover, the γ-irradiation analysis shows that the free electron spin is delocalized over physical entities formed of n elemen-

tary structures $(\alpha_1\beta_1\text{Spir}_1\text{Bchl}_2)_n$ where the most probable value of n is 6. It is important to realize that these larger aggregates must be discrete physical structures. They cannot be purely statistical entities delimited by proximity relationships in a sea of elementary structures. Otherwise, the Bernoulli statistics would not properly describe the linewidth versus survival probability relationship observed in Figs. 2, 4, and 5.

To be valid, this model must also be compatible with the observed target size of the species giving rise to the EPR signal. Fig. 3 compares the experimental survival of the signal as a function of the dose (solid line) with that predicted (dotted line) from oligomer $(\alpha_1\beta_1\text{Spir}_1\text{Bchl}_2)_6$ composed of elements with $M_r = 10{,}500$ (see legend to Fig. 3) and assuming one free electron per surviving oligomer $(\alpha_1\beta_1\text{Spir}_1\text{Bchl}_2)_k$ ($1 \leq k \leq 6$). According to this simulation, the surviving signal should not decay as a simple exponential function of the dose but should instead start decaying only when the number of surviving elements $(\alpha_1\beta_1\text{Spir}_1\text{Bchl}_2)$ is smaller than the initial number of oligomers $(\alpha_1\beta_1\text{Spir}_1\text{Bchl}_2)_6$. However, our experimental results show that the number of spins is directly proportional to the number of surviving elements. This means that ferricyanide assays for the number of elements in the system independently of their supramolecular association as oligomers. While each of the elements can react with ferricyanide, their rate of encounter with it seems to be limited by their number in the membrane. This number would, therefore, determine their reaction probability with ferricyanide. This assumption seems reasonable in view of the high ferricyanide/Bchl molar ratio required for unpaired spin generation (Fig. 1). As a consequence, the number of surviving spins at a given dose of γ-irradiation should—as is, in fact, observed (Fig. 3)—be a function of the target size of the elementary structure. Presumably, following the formation of Bchl^+, the sharing of the free electron modifies the redox potential of the remaining Bchl molecules of the oligomer, thus preventing any further oxidation by ferricyanide. This would prevent the formation of multiple radicals.

The discrete physical structures formed by the hexameric aggregates must force the 12 Bchl molecules to form closed assemblies that limit the mobility of the unpaired electron spin. This unpaired spin sharing may originate from a spin delocalization due to π–π orbital overlap between several Bchl molecules or to rapid electron hopping like that thought to occur in chlorophyll a water micelles (30). Although we cannot exclude a contribution from fast electron hopping, the gaussian lineshape of our EPR spectra and the large line narrowing observed in deuterated holochrome indicate hyperfine interaction as the most important line-narrowing factor.

While we cannot offer any definitive model, our data are compatible with a ringlike structure like that proposed for the photosynthetic membranes of Bchl b-containing *Rhodopseudomonas viridis* and *Ectothiorhodospira halochloris* (31–34). The latter structure was deduced by scanning transmission electron microscopy to be formed of a ring of six identical light-harvesting complexes, each containing three polypeptides with $(\alpha_2\beta_2\gamma_2)$ stoichiometry (34). These observations may not be directly applicable to *Rs. rubrum*, where no γ polypeptide has been reported. However, for holistic reasons it is tempting to assume that the two structures are fundamentally similar. Scanning electron transmission microscopy, which is sensitive to masses and to spatial orientation, and our γ-ray inactivation study, which is sensitive to pigment-associated masses, arrive at hexameric models: $(\alpha_1\beta_1\text{-Spir}_1\text{Bchl}_2)_6$ in *Rs. rubrum* and $(\alpha_2\beta_2\gamma_2)_6$ in *E. halochloris*.

In *Rs. rubrum*, we have no evidence to suggest that the photoreaction center has an organizing influence on the holochrome putative hexagonal structure. Indeed, the linewidth of the EPR signal is essentially the same in isolated B880 holochrome and in chromatophores from the wild-type strain S1 or from the reaction centerless strain F24 (17). It does not follow that these two pigment–protein complexes do not associate in the membrane: as we suggested earlier, the antenna polypeptides may considerably slow down the rotational motion of the photoreaction center in the plane of the membrane (35).

We thank Dr. Michael Potier from the Centre de Recherche Pédiatrique, Hôpital Sainte Justine, Université de Montréal, for the use of his ^{60}Co Gammacell. We also thank Dr. Ted Mar from this department for very helpful discussions. This work was made possible by a grant from the Natural Sciences and Engineering Council of Canada.

1. Vredenberg, W. J. & Amesz, J. (1966) *Biochim. Biophys. Acta* **126**, 244–253.
2. Thornber, J. P., Trosper, T. N. & Strouse, C. E. (1978) in *The Photosynthetic Bacteria*, eds. Clayton, R. K. & Sistrom, W. W. (Plenum, New York), pp. 113–160.
3. Cogdell, R. J., Zuber, H., Thornber, J. P., Drews, G., Gingras, G., Niederman, R. A., Parson, W. W. & Feher, G. (1985) *Biochim. Biophys. Acta* **806**, 185–186.
4. Cogdell, R. J., Lindsay, G., Valentine, J. & Durant, I. (1982) *FEBS Lett.* **150**, 151–154.
5. Picorel, R., Bélanger, G. & Gingras, G. (1983) *Biochemistry* **22**, 2491–2497.
6. Brunisholz, R. A., Cuendet, P. A., Theiler, R. & Zuber, H. (1981) *FEBS Lett.* **129**, 150–154.
7. Gogel, G. E., Parkes, P. S., Loach, P. A., Brunisholz, R. A. & Zuber, H. (1983) *Biochim. Biophys. Acta* **746**, 32–39.
8. Brunisholz, R. A., Suter, F. & Zuber, H. (1984) *Hoppe-Seyler's Z. Physiol. Chem.* **365**, 675–684.
9. Bélanger, G., Bérard, J. & Gingras, G. (1985) *Eur. J. Biochem.* **153**, 477–484.
10. Bérard, J., Bélanger, G., Corriveau, P. & Gingras, G. (1986) *J. Biol. Chem.* **261**, 82–87.
11. Picorel, R., L'Ecuyer, A., Potier, M. & Gingras, G. (1986) *J. Biol. Chem.* **261**, 3020–3024.
12. Peters, J. & Drews, G. (1983) *Eur. J. Cell Biol.* **29**, 115–120.
13. Niederman, R. A. & Gibson, K. D. (1978) in *The Photosynthetic Bacteria*, eds. Clayton, R. K. & Sistrom, W. W. (Plenum, New York), pp. 78–118.
14. Ueda, T., Morimoto, Y., Sato, M., Kakuno, T., Yamashita, J. & Horio, T. (1985) *J. Biochem.* **98**, 1487–1498.
15. Miller, J. F., Hinchigeri, S. B., Parkes-Loach, P. S., Callahan, P. M., Sprinkle, J. R., Riccobono, J. R. & Loach, P. A. (1987) *Biochemistry* **26**, 2055–2062.
16. Ghosh, R., Hauser, H. & Bachofen, R. (1988) *Biochemistry* **27**, 1004–1014.
17. Picorel, R., Lefebvre, S. & Gingras, G. (1984) *Eur. J. Biochem.* **142**, 305–311.
18. Picorel, R., del Campo, F. F., Ramirez, J. M. & Gingras, G. (1980) *Biochim. Biophys. Acta* **593**, 76–84.
19. Lascelles, J. (1956) *Biochem. J.* **62**, 78–93.
20. Vadeboncoeur, C., Noel, H., Poirier, L., Cloutier, Y. & Gingras, G. (1979) *Biochemistry* **18**, 4301–4308.
21. Beauregard, G., Giroux, S. & Potier, M. (1983) *Anal. Biochem.* **132**, 362–364.
22. McElroy, J. D., Feher, G. & Mauzerall, D. C. (1969) *Biochim. Biophys. Acta* **172**, 180–183.
23. Norris, J. R., Uphaus, R. A., Crespi, H. L. & Katz, J. J. (1971) *Proc. Natl. Acad. Sci. USA* **68**, 625–628.
24. Kepner, G. R. & Macey, R. I. (1968) *Biochim. Biophys. Acta* **163**, 188–203.
25. Norris, J. R. & Katz, J. J. (1978) in *The Photosynthetic Bacteria*, eds. Clayton, R. K. & Sistrom, W. W. (Plenum, New York), pp. 397–418.
26. Deisenhofer, J., Epp, O., Miki, K., Huber, R. & Michel, H. (1984) *J. Mol. Biol.* **180**, 385–398.
27. Allen, J. P., Feher, G., Yeats, T. O., Komiya, H. & Rees, D. C. (1987) *Proc. Natl. Acad. Sci. USA* **84**, 5730–5734.
28. Wasielewski, M. R. & Norris, J. R. (1981) *J. Am. Chem. Soc.* **103**, 7664–7665.
29. Wasielewski, M. R., Norris, J. R., Shipman, L. L., Lin, C. & Svec, W. A. (1981) *Proc. Natl. Acad. Sci. USA* **78**, 2957–2961.
30. Bowman, M. K., Michalski, T. J., Tyson, R. L., Worcester, D. L. & Katz, J. J. (1988) *Proc. Natl. Acad. Sci. USA* **85**, 1498–1502.
31. Miller, K. R. (1982) *Nature (London)* **300**, 53–55.
32. Welte, W. & Kreutz, W. (1982) *Biochim. Biophys. Acta* **692**, 479–488.
33. Stark, W., Kühlbrandt, W., Wildhaber, I. & Mühlethaler, K. (1984) *EMBO J.* **3**, 777–783.
34. Engelhardt, H., Engel, A. & Baumeister, W. (1986) *Proc. Natl. Acad. Sci. USA* **83**, 8972–8976.
35. Mar, T., Picorel, R. & Gingras, G. (1981) *Biochim. Biophys. Acta* **637**, 546–550.